Science Bulletin 64 (2019) 410–416

Contents lists available at ScienceDirect

Science Bulletin

journal homepage: www.elsevier.com/locate/scib

Article

NIR-II fluorescence in vivo confocal microscopy with aggregation-induced emission dots

Wenbin Yu [a,1], Bing Guo [b,1], Hequn Zhang [a], Jing Zhou [a], Xiaoming Yu [c], Liang Zhu [d], Dingwei Xue [c], Wen Liu [a], Xianhe Sun [a], Jun Qian [a,e,*]

[a] State Key Laboratory of Modern Optical Instrumentations, Centre for Optical and Electromagnetic Research, College of Optical Science and Engineering, Zhejiang University, Hangzhou 310058, China
[b] Department of Chemical and Biomolecular Engineering, National University of Singapore, Singapore 117585, Singapore
[c] Department of Urology, Sir Run-Run Shaw Hospital College of Medicine, Innovation Center for Minimally Invasive Technique and Device, Zhejiang University, Hangzhou 310016, China
[d] Interdisciplinary Institute of Neuroscience and Technology (ZIINT), Zhejiang University, Hangzhou 310058, China
[e] Joint Research Laboratory of Optics of Zhejiang, Normal University and Zhejiang University, Zhejiang Normal University, Jinhua 321000, China

ARTICLE INFO

Article history:
Received 21 January 2019
Received in revised form 15 February 2019
Accepted 18 February 2019
Available online 23 February 2019

Keywords:
Confocal microscopy
NIR-II fluorescence
AIE dots
In vivo cerebrovascular imaging
TCSPC
FLIM imaging

ABSTRACT

Significantly reduced tissue scattering of fluorescence signals in the second near-infrared (NIR-II, 1,000–1,700 nm) spectral region offers opportunities for large-depth in vivo bioimaging. Nowadays, most reported works concerning NIR-II fluorescence in vivo bioimaging are realized by wide-field illumination and 2D-arrayed detection (e.g., via InGaAs camera), which has high temporal resolution but limited spatial resolution due to out-of-focus signals. Combining NIR-II fluorescence imaging with confocal microscopy is a good approach to achieve high-spatial resolution visualization of biosamples even at deep tissues. In this presented work, a NIR-II fluorescence confocal microscopic system was setup. By using a kind of aggregation-induced emission (AIE) dots as NIR-II fluorescent probes, 800 μm-deep 3D in vivo cerebrovascular imaging of a mouse was obtained, and the spatial resolution at 700 μm depth could reach 8.78 μm. Moreover, the time-correlated single photon counting (TCSPC) technique and femtosecond laser excitation were introduced into NIR-II fluorescence confocal microscopy, and in vivo confocal NIR-II fluorescence lifetime microscopic imaging (FLIM) of mouse cerebral vasculature was successfully realized.

1. Introduction

As a kind of promising method for biomedical research, in vivo fluorescence imaging provides ways to directly observe biological structure and dynamic physiological process with high spatial and temporal resolution [1]. Previous studies show that compared to conventional in vivo fluorescence imaging whose emission is in the visible and near-infrared window of 400–900 nm, in vivo fluorescence imaging in the second near-infrared (NIR-II, 1,000–1,700 nm) spectral region has drawn much attention due to the significantly reduced optical scattering of emission signals in biological tissues [2–4]. Thus far most reported works on NIR-II fluorescence in vivo imaging were realized via the mode of wide-field illumination and 2D-arrayed detection (e.g., using a InGaAs camera to record the images) [5–7]. These imaging modalities usually have high temporal resolution and large imaging depth. However, the spatial resolution is usually limited, since the out-of-focus signal usually superimposes onto the in-focus signal and thus blurs the whole image.

Fluorescence confocal microscopy relies on point-by-point excitation and single-point detection, and it possesses the advantage of high spatial resolution thanks to the existence of pinhole. In the confocal structure, a pinhole locates at the conjugation position corresponding to the focal point. Thus, only the signal from a small probe volume at the focusing spot can pass through the pinhole and further be detected by the photodetector (e.g., photomultiplier diode (PMT)). In this way, out-of-focus signals can be rejected, endowing confocal microscopy with optical sectioning capability of samples and high spatial resolution. Nowadays, conventional fluorescence confocal microscopy has been mature. However, its imaging depth is still limited since the wavelength of excitation and emission light usually locate in 400–700 nm, where light has intense tissue absorption and scattering [8,9].

* Corresponding author.
E-mail address: qianjun@zju.edu.cn (J. Qian).
[1] These authors contributed equally to this work.

https://doi.org/10.1016/j.scib.2019.02.019
2095-9273/

Fluorescence bioimaging usually requires exogenous probes. Nano-materials have promoted the development of various new devices and technologies during the past decades [10–13]. So far, many kinds of nanosized NIR-II fluorescent probes (e.g., quantum dots, carbon nanotubes, and rare-earth doped nanoparticles), as well as their related biological applications, have been reported [14–16]. However, considering the biosafety issue, organic fluorescent nanoprobes are more suitable for functional bioimaging [17]. Most of the conventional organic fluorophores have very weak or no emission when they form nanoparticles, since they have the characteristic of aggregation-caused quenching (ACQ) [18]. Aggregation-induced emission (AIE) is a kind of phenomenon opposite to ACQ [19–21]. When AIE luminogens (AIEgens) are encapsulated to organic dots, their brightness can be simply enhanced by increasing the amount of doped AIEgens inside. Thus, AIE dots are promising candidates for fluorescence bioimaging [22–24]. Previously, AIE dots were mainly employed for in vitro and in vivo biomedical applications, based on their visible and NIR-I (700–900 nm) emission [22]. Very recently, AIE dots have been applied in NIR-II fluorescence whole-body in vivo imaging and wide-field microscopic in vivo imaging [7,25,26].

In this work, to increase the tissue penetration capability of confocal microscopy, or in other words to improve the spatial resolution of NIR-II fluorescence imaging, we combined these two kinds of technologies together and established a NIR-II fluorescence confocal microscope. Based on this setup, AIE dots were firstly utilized for NIR-II fluorescence confocal microscopic imaging of intravital animal, and 3D cerebrovascular imaging of mice with large-depth and high-spatial resolution was achieved. In addition, fluorescence lifetime imaging technology was introduced to the NIR-II fluorescence confocal microscopy, and AIE dots assisted in vivo confocal NIR-II fluorescence lifetime microscopic imaging was successfully demonstrated.

2. Experimental

2.1. Material

The synthesis of donor-acceptor (D-A) tailored NIR-II emissive AIEgen (TB1), as well as its encapsulation process to organic AIE dots (TB1 dots), was referred to our previously published work [26].

2.2. Basic experimental instruments

Absorption spectra were tested with a Shimadzu Model UV-1700 spectrometer. Photoluminescence (PL) spectra were taken by a fluorescence spectrometer (F900, Edinburgh Instruments Ltd.). The average size of AIE dots was measured by dynamic light scattering (DLS).

2.3. Home-built NIR-II fluorescence confocal microscope

In brief, a collimated 793 nm laser (maximum output power: 10W; Suzhou Rugkuta Optoelectronics Co., Ltd.) was used as the excitation source. The beam was guided onto a 900 nm long-pass dichroic mirror, and then reflected to the scanning galvanometer (average reflectance between 1,080 and 1,700 nm: >97%; scanning speed: 10 μs/pixel; scanning area: 512 pixels×512 pixels), which controls the scanning process of laser focal point in the *x-y* directions. After passing through the scan lens, tube lens and an objective with near infrared anti-reflection film, the 793 nm excitation beam was eventually focused on the sample (could be ex vivo tissue slices or an in vivo mouse brain with the cranial window in our experiments). NIR-II fluorescence from the sample passed back through the same objective in the opposite direction, and was allowed to pass through the 900 nm long-pass dichroic mirror and a 1000 nm long-pass filter. The fluorescence above 1000 nm was then focused onto an optical fiber (diameter of core: ~300 μm) by an optical collimator with near infrared anti-reflection film. Then, fluorescence signal guided in the fiber was focused onto a NIR (950–1,700 nm) sensitive PMT (H12397-75, Hamamatsu). The electrical signal generated in the PMT was amplified by an electrical signal amplifier (C12319, Hamamatsu), based on which an image could be reconstructed via a computer.

2.4. Confocal NIR-II fluorescence lifetime microscopic imaging (FLIM) system

In brief, an 810-nm femtosecond pulsed laser (Mantis-5 Titanium-Sapphire Oscillator; Average output power: 480 mW; repetition rate: 80 MHz; FWHM: 84 nm; COHERENT) beam was guided into a commercial confocal microscope (FV1000+BX61, Olympus) as the excitation source. NIR-II fluorescence signal from the sample was detected by the NIR (950–1,700 nm) sensitive PMT (H12397-75, Hamamatsu). The time-correlated single photon counting module system (TCSPC, SPC-150, Becker & Hickl GmbH) integrated in a computer then constructed the NIR-II FLIM image, according to the synchronous signals from a photodiode (PD) and the scanning unit, as well as the electric signals from the PMT (amplified by a high speed amplifier, C5594, Hamamatsu).

2.5. Experimental animal

Institute of Cancer Research (ICR) mice (6–7 weeks old, female) were selected as experimental animals. They were provided from the SLAC laboratory Animal Co. Ltd. (Shanghai, China) and housed in the Laboratory Animal Center of Zhejiang University (Hangzhou, China). The animal housing area was maintained at 24 °C with a 12 h light/dark cycle, and animals were fed with water and standard laboratory chow. "The National Regulation of China for Care and Use of Laboratory Animals" was strictly followed and all in vivo experiments were approved by the Institutional Ethical Committee of Animal Experimentation Zhejiang University. The skulls of mice were opened up through microsurgery after they were anesthetized. A round thin cover glass slide was then mounted onto the mouse brain and directly adhered to it through dental cement. The purpose for mounting the cover glass slide is to protect and flatten the mouse brain, ensuring the microscopic imaging quality [27]. The anesthetized mouse with the cranial window was intravenously injected with 400 μL 1×phosphate buffered saline (PBS) dispersion of TB1 dots (2 mg/mL), and the head of mouse was immobilized before brain angiography.

3. Results and discussions

The setup of our home-built NIR-II fluorescence confocal microscope was shown in Fig. 1. The sample focal plane and the end face of optical fiber were adjusted as a pair of conjugated planes. Thus, the fiber played the role of pinhole, whose size was ~300 μm (approximated to the diameter of fiber core). Overall, in the NIR-II fluorescence confocal microscope, the selected optical components should be infrared anti-reflection and the optical path should be as short as possible, to ensure enough signal excitation and collection efficiency.

Herein, a kind of AIEgen named TB1 was utilized (Fig.1a), and Fig. 2b shows the encapsulation process of TB1 dots [26]. The aqueous dispersion of TB1 dots was clear and transparent (inset of Fig. 2c), and the average particle size was ~37 nm (Fig. 2c). As shown in Fig. 2d, TB1 dots showed an absorption peak at 740 nm,

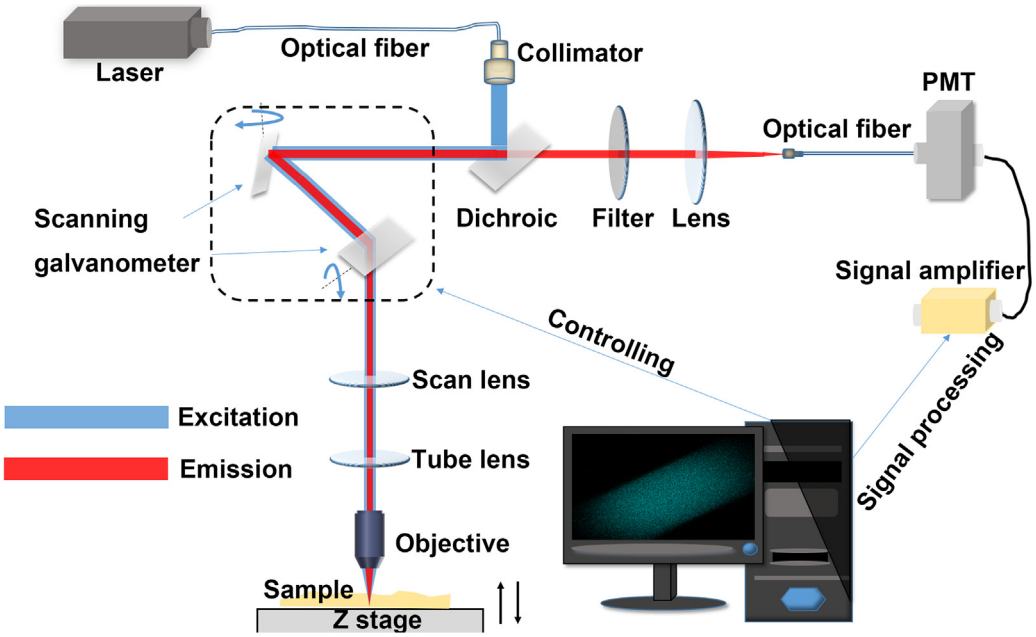

Fig. 1. (Color online) A simplified optical diagram of the galvanometer scanning based NIR-II fluorescence confocal microscope.

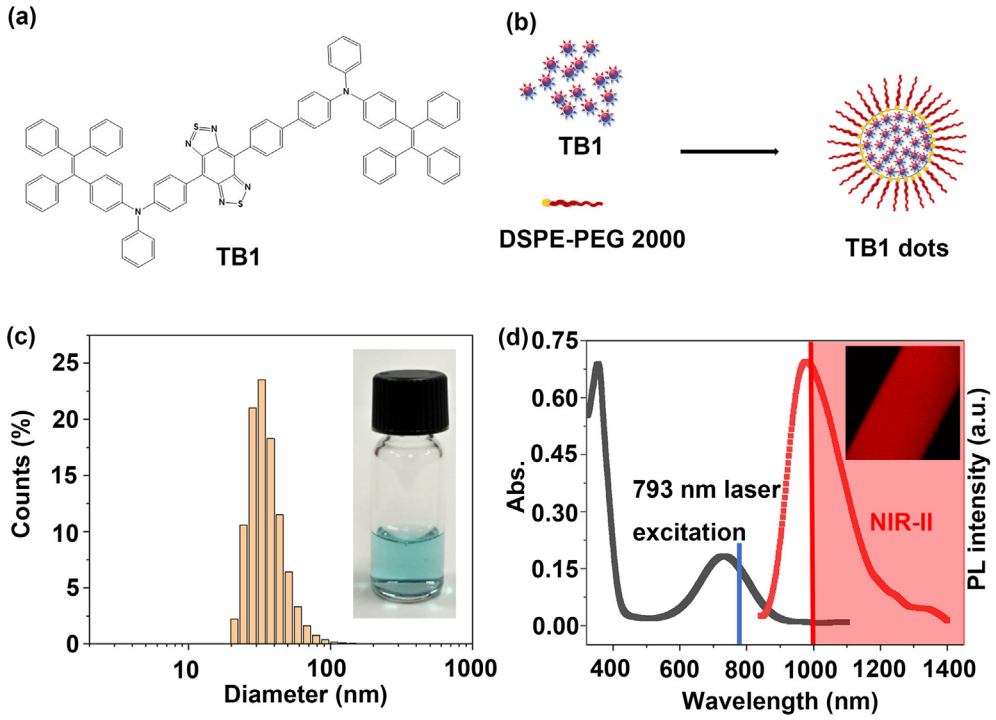

Fig. 2. (Color online) Characterizations of TB1 dots. (a) The molecular structure of AIEgen named TB1. (b) The encapsulation process of TB1 dots. (c) The size distribution of TB1 dots, measured by DLS. Inset: the photograph of TB1 dots in aqueous dispersion under daylight. (d) Absorption and fluorescence spectra of TB1 dots. Inset: the NIR-II fluorescence confocal microscopic image of a glass capillary tube, which was filled with the aqueous dispersion of TB1 dots (1 mg/mL).

and the absorbance at 793 nm was about 8.2 L/(g cm). The TB1 dots had an emission peak at 975 nm, and a large tail extended beyond 1,000 nm. According to our previous work, NIR-II fluorescence quantum yield (QY) of the dots was as high as 6.2% [26]. Thus, TB1 dots exhibited bright signal, under the home-built NIR-II fluorescence confocal microscopic system (inset of Fig. 2d). In addition, TB1 dots demonstrated low cytotoxicity and good hemocompatibility [26].

To evaluate the performance of the as-established NIR-II fluorescence confocal microscope, ex vivo imaging of tissue slices was firstly conducted and the most representative results were shown in Fig. 3. Bright fluorescent spots were observed on the tissue slices, which were harvested from the mice 24 h post the intravenous injection of TB1 dots. In contrast, nothing could be observed on the tissue slices of the mice in the control group. The results illustrate that the fluorescent spots should arise from

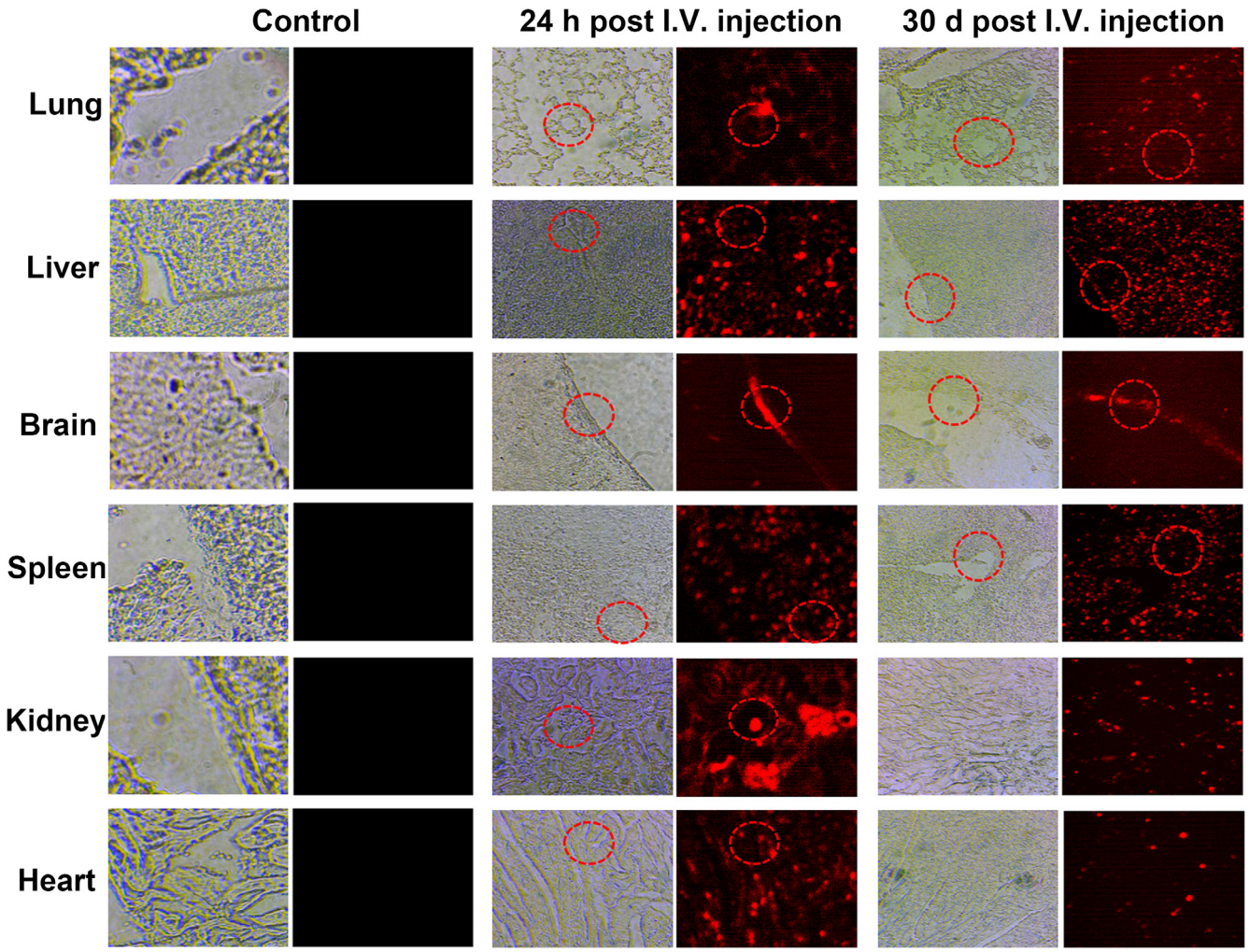

Fig. 3. (Color online) Representative ex vivo NIR-II fluorescence confocal microscopic images (25X water objective, 793 nm excitation, emission >1,000 nm) of various types of tissues slices. Animal models: three groups of 2 weeks-old female mice. Group 1: control group, mice without any treatment; group 2 and 3: mice injected with TB1 dots (2 mg/mL, 200 μL) through the tail vein (I.V. injection) and fed normally for another 24 h (group 2) and 30 d (group 3), respectively.

the TB1 dots, which accumulated in the organs of the treated mice after intravenous injection. For the mice 30 d post the treatment, the distributions of dots in the tissue slices of lung, liver, brain and spleen were similar as those of mice 24 h post the treatment, indicating the clearance of dots in these organs was slow. However, in the tissue slices of kidney and heart, the quantities of fluorescent spots got significant decrease, suggesting TB1 dots experienced certain excretion in these organs. Thus, NIR-II fluorescence confocal microscopy holds the potentials for studying the distribution and biological metabolic process of other kinds of NIR-II fluorescent agents in future. Furthermore, before the TB1 dots treated mice were sacrificed, physical and neurological evaluations on them (compared with healthy and non-treated mice) were also conducted. No changes in weight, shape, eating, drinking, exploratory behavior or activity were observed from mice 30 d post the injection of dots, illustrating TB1 dots possessed good biocompatibility.

In vivo NIR-II fluorescence confocal microscopic imaging was further conducted. Fast scanning in a certain vertical depth of the mouse brain were achieved using the galvanometer at a speed of 10 μs/pixel, and the axial scanning (in depth direction) was achieved by an electric displacement stage with a step of 10 μm. The scanning area was set to be 512 pixels × 512 pixels (0.94 μm/pixel). In this way, tomographic fluorescence images with high spatial resolution could be obtained. Fig. 4a shows representative imaging results, and the cerebral blood vessels of the mouse at various vertical depths below the skull could be clearly visualized. Owing to the low tissue absorption of 793 nm excitation light and low tissue scattering of NIR-II fluorescence, the imaging depth reached >800 μm. In addition, tiny capillary vessels (diameter = 5.77 μm at the depth of 350 μm and diameter = 8.78 μm at the depth of 700 μm) could be distinguished easily (Fig. 4b and c), thanks to the high spatial resolution feature of NIR-II fluorescence confocal microscope. By reconstructing the images recorded at various depths of the brain, a vivid 3D cerebrovascular architecture was obtained (Fig. 4d and e). To the best of our knowledge, this is the first example about the application of AIE dots for NIR-II fluorescence in vivo confocal microscopy. The imaging depth and resolution of our NIR-II fluorescence confocal microscopy could be comparable to those of two-photon fluorescence microscopy, which is currently the dominant approach for intravital optical imaging. However, two-photon fluorescence microscopy relies on an expensive femtosecond laser as the excitation source. In addition, dispersion should be controlled carefully to compress the pulse width of laser as narrow as possible, achieving high peak power of laser beam, as well as effective two-photon excitation. In contrast, a cost-effective and facilely operated continuous wave (CW) laser was adopted as the source in our NIR-II fluorescence

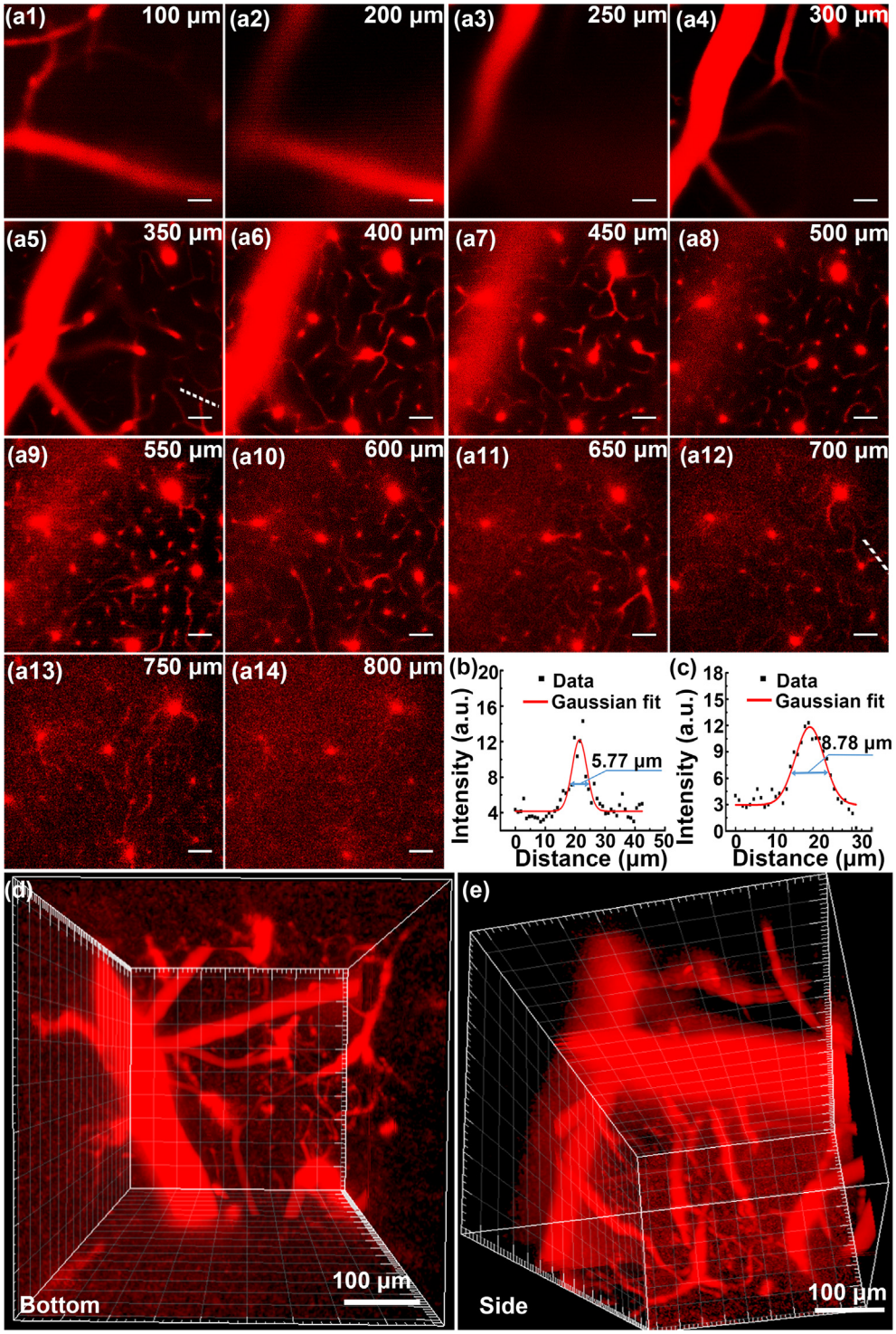

Fig. 4. (Color online) In vivo NIR-II fluorescence confocal microscopic imaging. (a1–a14) In vivo NIR-II fluorescence confocal scanning microscopic images of mouse brain vasculature at various depths (793 nm excitation, emission >1,000 nm, laser power ~70 mW, PMT voltage ~600 V). Scale bar: 50 μm. (b) and (c) The cross-sectional intensity profiles along the capillary vessels indicated by the white-dashed lines in (a5 and a12). The Gaussian fits to the profiles are shown in curves. (b) The Gaussian fit to the profile at 350 μm depth. (c) The Gaussian fit to the profile at 700 μm depth. (d) and (e) 3D reconstruction of vasculatures in brain with 800 μm depth: (d) bottom view, (e) side view.

confocal microscopy. It also has better bio-safety than the high-peak-intensity femtosecond laser, which may modulate the biological activities and dynamics [28,29]. Furthermore, it is worth noting that a faster scanning speed (10 μs/pixel) was achieved in our intravital NIR-II fluorescence confocal microscopic imaging, compared to that (50 μs/pixel) in a recently published literature [30].

The combination of fluorescence confocal microscopy and time-correlated single photon counting technique (TCSPC) is a conventional way to realize FLIM imaging [31–33]. In this work, we set up the NIR-II FLIM system (Fig. 5a). The photon counting time of an image was 40 s. In other words, the FLIM imaging speed was 40 s/frame. We first utilized this system to perform the imaging

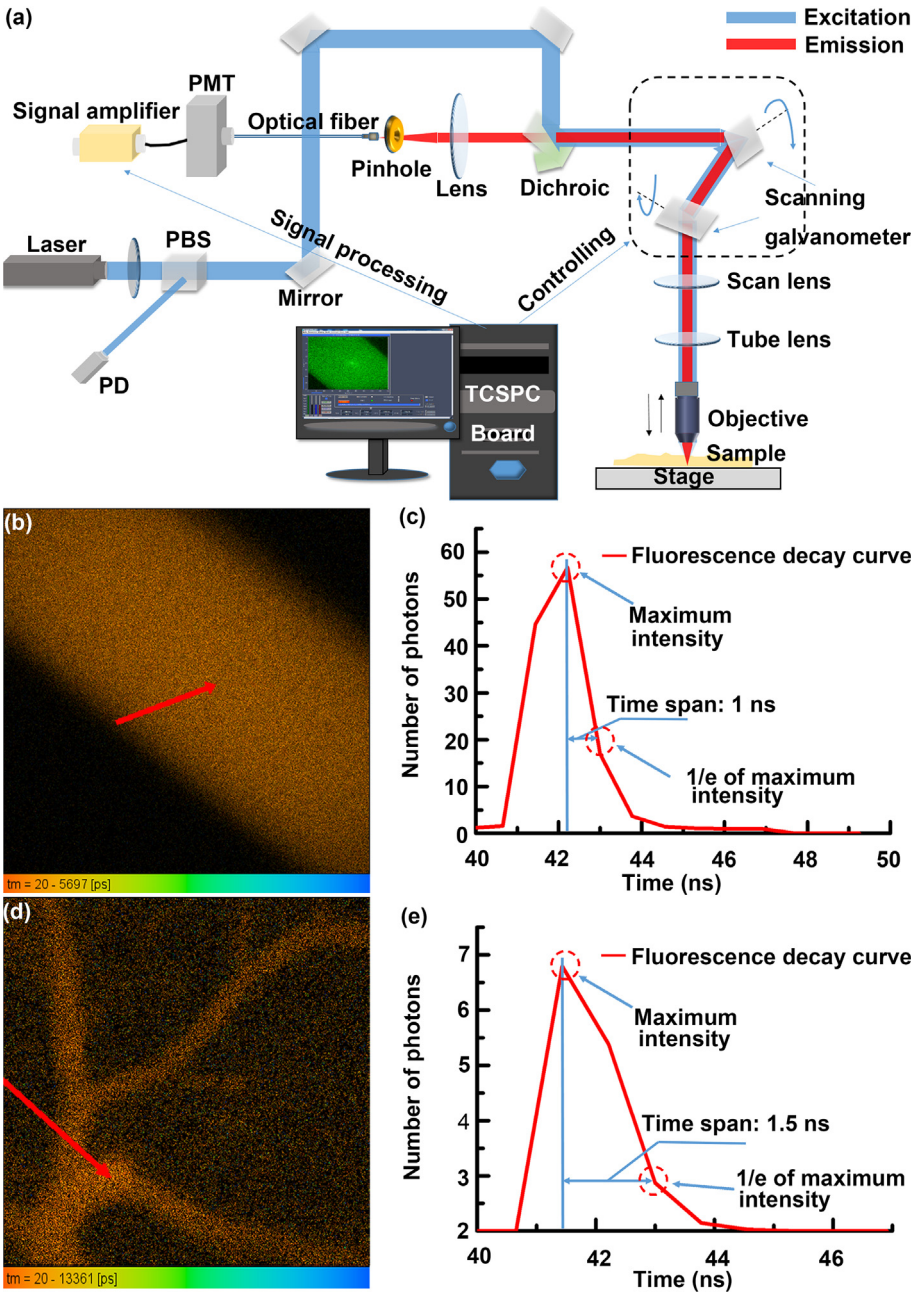

Fig. 5. (Color online) In vivo confocal NIR-II fluorescence lifetime microscopic imaging. (a) A simplified optical diagram of confocal NIR-II fluorescence lifetime microscopic imaging system. (b) A NIR-II FLIM image of the glass capillary tube filled with TB1 dots (1 mg/mL). (c) Fluorescence decay curve measured at the arrow in (b), showing the fluorescence lifetime of TB1 dots is 1 ns. (d) An in vivo NIR-II FLIM image of cerebral vessels in mouse, which was intravenously injected with TB1 dots (2 mg/mL, 400 μL). (e) Fluorescence decay curve measured at the arrow in (d), showing the fluorescence lifetime of TB1 dots in vessels is 1.5 ns. Imaging parameters: 810 nm excitation, emission >1,000 nm, laser power ~50 mW, PMT voltage ~600 V.

of TB1 dots in aqueous dispersion (Fig. 5b), and the NIR-II fluorescence lifetime was measured as 1 ns (Fig. 5c). Herein, fluorescence lifetime was calculated by measuring the time span between the time point when the fluorescence intensity was maximum and the time point when the fluorescence intensity decreased to 1/e of the maximum intensity in the fluorescence decay curve. Furthermore, in vivo NIR-II FLIM cerebrovascular imaging of a mouse (injected with dots) was conducted, and the structure of cerebral vasculature at one vertical depth was visualized (Fig. 5d), where the NIR-II fluorescence lifetime was about 1.5 ns (Fig. 5e). As far as we know, this is the first demonstration of intravital NIR-II FLIM imaging.

4. Conclusions

In summary, by employing a home-built NIR-II fluorescence confocal microscopic system and a kind of AIE organic dots, 800 μm-deep 3D in vivo cerebrovascular imaging of a mouse with high spatial resolution was achieved. Moreover, based on a confocal microscope, a femtosecond pulsed laser and the TCSPC technology, in vivo NIR-II FLIM imaging of mouse cerebral vasculature was demonstrated for the first time. Future works may focus on optimizing the NIR-II FLIM setup and seeking more biocompatible NIR-II fluorescent probes, achieving in vivo 4D (3D+ lifetime) brain functional imaging.

Conflict of interest

The authors declare that they have no conflict of interest.

Acknowledgments

We sincerely thank Prof. Bin Liu from the Department of Chemical and Biomolecular Engineering in National University for providing the TB1 dots and helpful discussion. This work was supported by the National Natural Science Foundation of China (61735016) and Zhejiang Provincial Natural Science Foundation of China (LR17F050001).

Author contributions

Wenbin Yu was mainly responsible for the design and operation of imaging experiments. Bing Guo mainly designed and synthesized TB1 dots. Wenbin Yu and Bing Guo contributed equally to this work. Hequn Zhang, Jing Zhou and Wen Liu assisted with imaging experiments. Liang Zhu completed craniotomy on mice. Xiaoming Yu and Dingwei Xue anesthetized and fixed mice. Xianhe Sun gave some assistance in writing. Jun Qian was the corresponding author of this article, designed the imaging systems and provided guidance in the entire research process.

References

[1] Ellenbroek SIJ, van Rheenen J. Imaging hallmarks of cancer in living mice. Nat Rev Cancer 2014;14:406–18.
[2] Diao S, Blackburn JL, Hong GS, et al. Fluorescence imaging in vivo at wavelengths beyond 1,500 nm. Angew Chem Int Ed 2015;54:14758–62.
[3] Diao S, Hong GS, Antaris AL, et al. Biological imaging without autofluorescence in the second near-infrared region. Nano Res 2015;8:3027–34.
[4] Wang R, Li XM, Zhou L, et al. Epitaxial seeded growth of rare-earth nanocrystals with efficient 800 nm near-Infrared to 1,525 nm short-wavelength infrared downconversion photoluminescence for in vivo bioimaging. Angew Chem Int Ed 2014;53:12086–90.
[5] Hong GS, Diao S, Chang JL, et al. Through-skull fluorescence imaging of the brain in a new near-infrared window. Nat Photon 2014;8:723–30.
[6] Antaris AL, Chen H, Cheng K, et al. A small-molecule dye for NIR-II imaging. Nat Mater 2016;15:235–42.
[7] Alifu N, Zebibula A, Qi J, et al. Single-molecular near-infrared-ii theranostic systems: ultrastable aggregation-induced emission nanoparticles for long-term tracing and efficient photothermal therapy. ACS Nano 2018;12:11282–93.
[8] Englhard AS, Palaras A, Volgger V, et al. Confocal laser endomicroscopy in head and neck malignancies using FITC-labelled EpCAM- and EGF-R-antibodies in cell lines and tumor biopsies. J Biophoton 2017;10:1365–76.
[9] Goetz M, Deris I, Vieth M, et al. Near-infrared confocal imaging during mini-laparoscopy: a novel rigid endomicroscope with increased imaging plane depth. J Hepatol 2010;53:84–90.
[10] Prasad PN. Introduction to nanomedicine and nanobioengineering. New Jersey: Wiley John & Sons; 2012.
[11] Zhou L, Guang Z, Rusen Y, et al. Muscle-driven in vivo nanogenerator. Adv Mater 2010;22:2534–7.
[12] Zheng Q, Shi B, Fan F, et al. In vivo powering of pacemaker by breathing-driven implanted triboelectric nanogenerator. Adv Mater 2014;26:5851–6.
[13] Zhen Q, Zou Y, Zhang Y, et al. Biodegradable triboelectric nanogenerator as a life-time designed implantable power source. Sci Adv 2016;2:e1501478.
[14] Zebibula A, Alifu N, Xia LQ, et al. Ultrastable and biocompatible NIR-II quantum dots for functional bioimaging. Adv Funct Mater 2018;28:1703451.
[15] Hong GS, Lee JC, Robinson JT, et al. Multifunctional in vivo vascular imaging using near-infrared II fluorescence. Nat Med 2012;18:1841–6.
[16] Naczynski DJ, Tan MC, Zevon M, et al. Rare-earth-doped biological composites as in vivo shortwave infrared reporters. Nat Commun 2013;4:2199.
[17] Hong GS, Zou YP, Antaris AL, et al. Ultrafast fluorescence imaging in vivo with conjugated polymer fluorophores in the second near-infrared window. Nat Commun 2014;5:4206.
[18] Birks JB. Photophysics of aromatic molecules. London: Wiley; 1970.
[19] Luo JD, Xie ZL, Lam JWY, et al. Aggregation-induced emission of 1-methyl-1,2,3,4,5-pentaphenylsilole. Chem Commun 2001;18:1740–1.
[20] Zong L, Gong Y, Yu Y, et al. New perylene diimide derivatives: stable red emission, adjustable property from ACQ to AIE, and good device performance with an EQE value of 4.93%. Sci Bull 2018;63:108–16.
[21] Wang C, Li L, Zhan XJ, et al. Blue AIEgens bearing triphenylethylene peripheral: adjustable intramolecular conjugation and good device performance. Sci Bull 2016;61:1746–55.
[22] Qian J, Tang BZ. AIE luminogens for bioimaging and theranostics: from organelles to animals. Chem 2017;3:56–91.
[23] Mei J, Leung NL, Kwok RT, et al. Aggregation-induced emission: together we shine, united we soar! Chem Rev 2015;115:11718–940.
[24] Cai X, Bandla A, Mao D, et al. Biocompatible red fluorescent organic nanoparticles with tunable size and aggregation-induced emission for evaluation of blood-brain barrier damage. Adv Mater 2016;28:8760–5.
[25] Qi J, Sun C, Zebibula A, et al. Real-time and high-resolution bioimaging with bright aggregation-induced emission dots in short-wave infrared region. Adv Mater 2018;30:1706856.
[26] Sheng ZH, Guo B, Hu DH, et al. Bright aggregation-induced-emission dots for targeted synergetic NIR-II fluorescence and NIR-I photoacoustic imaging of orthotopic brain tumors. Adv Mater 2018;30:e1800766.
[27] Qian J, Wang D, Cai FH, et al. Observation of multiphoton-induced fluorescence from graphene oxide nanoparticles and applications in in vivo functional bioimaging. Angew Chem Int Ed 2012;51:10570–5.
[28] Wang SY, Liu YH, Zhang DP, et al. Photoactivation of extracellular-signal-regulated kinase signaling in target cells by femtosecond laser. Laser Photon Rev 2018;12:1700137.
[29] He H, Li S, Wang S, et al. Manipulation of cellular light from green fluorescent protein by a femtosecond laser. Nat Photon 2012;6:651–6.
[30] Wan H, Yue JY, Zhu SJ, et al. A bright organic NIR-II nanofluorophore for three-dimensional imaging into biological tissues. Nat Commun 2018;9:1171.
[31] Becker W, Bergmann A, Konig K, et al. Picosecond fluorescence lifetime microscopy by TCSPC imaging. Multiphoton Microscopy Biomed Sci 2001;1:414–9.
[32] Becker W, Bergmann A, Hink MA, et al. Fluorescence lifetime imaging by time-correlated single-photon counting. Microsc Res Tech 2004;63:58–66.
[33] Duncan RR, Bergmann A, Cousin MA, et al. Multi-dimensional time-correlated single photon counting (TCSPC) fluorescence lifetime imaging microscopy (FLIM) to detect FRET in cells. J Microsc 2004;215:1–12.

Wenbin Yu is a master candidate student of the Centre for Optical and Electromagnetic Research of Zhejiang University. He received his Bachelor's degree in Changchun University of Science and Technology. His current research fields lie in biophotonics.

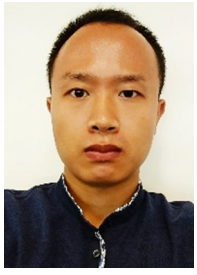

Bing Guo received his bachelor and M.Phil. degrees from the Zhengzhou University and The Hong Kong Polytechnic University, respectively. He continued to study for his Ph.D. degree and work as a research fellow at Prof. Liu Bin's group in National University of Singapore. Recently, his research has been focused on developing novel organic nanomaterials for optical brain imaging and therapy in the second near-infrared window.

Jun Qian received his bachelor and Ph.D. degrees from the Department of Optical Engineering of Zhejiang University in 2004 and 2009, respectively. He worked at Prof. Paras Prasad's Group in the University at Buffalo as a visiting scholar during 2006–2007. He is now a professor in the College of Optical Science and Engineering, Zhejiang University. His research focuses on nano-biophotonics, especially nanoparticle-assisted optical functional bioimaging.